An improved version of a high accuracy surface modeling method

Na Zhao, Tianxiang Yue & Mingwei Zhao

GEM - International Journal on Geomathematics

ISSN 1869-2672
Volume 4
Number 2

Int J Geomath (2013) 4:185-200
DOI 10.1007/s13137-013-0051-z

Int J Geomath (2013) 4:185–200
DOI 10.1007/s13137-013-0051-z

ORIGINAL PAPER

An improved version of a high accuracy surface modeling method

Na Zhao · Tianxiang Yue · Mingwei Zhao

Received: 17 April 2013 / Accepted: 16 September 2013 / Published online: 4 October 2013

Abstract A method of surface modeling, high accuracy surface modeling (HASM), which is based on the fundamental theorem of surface theory, is modified. The earlier version of HASM is theoretically incomplete and almost performs similar or slightly better than other methods being compared in the practical applications which definitely limit its promotion. According to the fundamental theorem of surface theory, we modify HASM by adding another important nonlinear equation to solve the low accuracy in some cases and make HASM have a complete and solid theory foundation. A numerical test and a real-world example are employed to comparatively validate the effectiveness of this modification. It is found that the accuracy of the simulation result has a great improvement. Another feature of the modified version of HASM is that it is theoretically perfect since it considers the third equation of the surface theory. The modified HASM will be useful with a wide range of spatial interpolation, particularly if the focus on simulation accuracy.

Keywords HASM · Interpolation method · Discrete schemes · Accuracy · Temperature

Mathematics Subject Classification 53A05 · 35G20 · 35C99

N. Zhao · T. Yue (✉)· M. Zhao
State Key Laboratory of Resources and Environmental Information System,
Institute of Geographic Sciences and Natural Resources Research,
Chinese Academy of Sciences, Beijing 100101, China
e-mail: yue@lreis.ac.cn

N. Zhao
e-mail: zhaon@lreis.ac.cn

M. Zhao
e-mail: zhaomw@lreis.ac.cn

1 Introduction

The methods of surface modeling have been experienced rapid development since the first digital elevation model was developed and the error problem has become a major concern since the 1960s (Crain 1970; Li and Zhu 2000; Stott 1977). Although several improvement techniques are proposed, the error problem still exists which has long troubled surface modeling (Wise 2000). To find a solution for the error problems produced by geographical information, high accuracy surface modeling (HASM) method is thus developed by Yue (2011) in terms of the fundamental theorem of surface theory.

Researches on HASM can be divided into four informal stages: HASM1, HASM2, HASM3 and HASM4 (Yue 2011). Several methods are developed to solve the equations of the corresponding version of HASM, such as modified Gauss–Seidel method (MGS), preconditioned conjugate gradient method (PCG), adaptive method (AM) and multi-grid method (MG) (Yue et al. 2010a,b; Yue 2011; Chen et al. 2012). The accuracy of HASM4 with PCG method is higher than the previous versions (Yue and Du 2006; Yue and Wang 2010; Chen et al. 2012). Numerical tests have shown that HASM4 is usually much more accurate than the classical methods such as kriging, inverse distance weighting (IDW) method, and splines (Yue et al. 2007, 2010a,b). Surface modeling of digital elevation model, terrestrial ecosystems, ecological diversity, and soil properties also indicate that HASM has increased interpolation accuracy (Yue 2011). However, by doing more experiments, we found a phenomenon that HASM usually performs slightly better than other methods being compared in practical applications. Besides, there are also some cases, especially in climate research, indicating that the accuracy of HASM is not as good as kriging method even the initial values of HASM obtained by kriging method. Because of these, the widespread application of HASM is limited. In addition, HASM has not been publicly accepted by end-users since the theoretical basis of it is not complete and thus is not robust.

To completely resolve error problem of HASM and promote its application, the aim in this paper is to give an improved version of it in terms of the fundamental theorem of surface theory. This new model will be compared to the previous one (HASM4), where HASM4 employs only part of the partial differential equations of the surface theory. We denote the new version of HASM here and hereafter is Mod.HASM. In numerical experiments, Gauss synthetic surface is used to validate the new model. As an interesting and important application of the interpolation technique, in the real world examples, we apply Mod. HASM to simulate annual mean temperature of China during 1951–2010. Simulation accuracy of Mod.HASM is compared with that of the previous version (HASM4) and other classical methods: kriging, IDW and splines, which have been the most widely used in climate research.

2 The basic theory of HASM

As a new surface modeling method, HASM is based on the fundamental theorem of surface theory which makes sure that a surface is uniquely defined by the first and the second fundamental coefficients of it (Henderson 1998; Somasundaram 2005). In this section, the theoretical basis of HASM is given briefly.

The fundamental theorem of surface theory is as follows (Su and Hu 1997; Somasundaram 2005).

Theorem *When the coefficients of the two quadratic differential forms* $Edu^2 + 2Fdudv + Gdv^2$, $Ldu^2 + 2Mdudv + Ndv^2$, *are such that the first quadratic form is positive definite and the six coefficients* E, F, G, L, M, N *satisfy Gauss–Codazii equations, there exists a surface* $z = f(x, y)$ *uniquely determined by* (1) *under the given initial condition* $f(x, y) = f(x_0, y_0)(x = x_0, y = y_0)$.

$$\begin{cases} f_{xx} = \Gamma^1_{11} f_x + \Gamma^2_{11} f_y + \frac{L}{\sqrt{E+G-1}} \\ f_{yy} = \Gamma^1_{22} f_x + \Gamma^2_{22} f_y + \frac{N}{\sqrt{E+G-1}} \\ f_{xy} = \Gamma^1_{12} f_x + \Gamma^2_{12} f_y + \frac{M}{\sqrt{E+G-1}} \\ \frac{f_y f_{xy} + f_x f_{xx}}{(1+f_x^2+f_y^2)^{3/2}} = \frac{L}{E} f_x + \frac{M}{G} f_y \\ \frac{f_x f_{xy} + f_y f_{yy}}{(1+f_x^2+f_y^2)^{3/2}} = \frac{M}{E} f_x + \frac{N}{G} f_y \end{cases}, \tag{1}$$

where, $E = 1 + f_x^2, F = f_x \cdot f_y, G = 1 + f_y^2, L = \frac{f_{xx}}{\sqrt{1+f_x^2+f_y^2}}, M = \frac{f_{xy}}{\sqrt{1+f_x^2+f_y^2}}, N = \frac{f_{yy}}{\sqrt{1+f_x^2+f_y^2}}, \Gamma^1_{11} = \frac{GE_x - 2FF_x + FE_y}{2(EG-F^2)}, \Gamma^2_{11} = \frac{2EF_x - EE_y - FE_x}{2(EG-F^2)}, \Gamma^1_{22} = \frac{2GF_y - GG_x - FG_y}{2(EG-F^2)}, \Gamma^2_{22} = \frac{EG_y - 2FF_y + FG_x}{2(EG-F^2)}, \Gamma^1_{12} = \frac{GE_y - FG_x}{2(EG-F^2)}, \Gamma^2_{12} = \frac{EG_x - FE_y}{2(EG-F^2)}$, *and the Gauss–Codazii equations are*

$$\begin{cases} L_y - M_x = L\Gamma^1_{12} - N\Gamma^2_{11} + M(\Gamma^2_{12} - \Gamma^1_{11}) \\ M_y - N_x = L\Gamma^1_{22} - N\Gamma^2_{12} + M(\Gamma^2_{22} - \Gamma^1_{12}) \end{cases}. \tag{2}$$

E, F, G *are the first fundamental forms and indicate how the surface inherits the natural inner product of* R^3, *in which* R^3*is the set of triples* (x, y, z) *of real numbers* (*Carmo* 2006). *The coefficients of the first fundamental forms of a surface yield information about some geometric properties, which are called intrinsic geometric properties including angles of tangent vectors, the lengths of curves, the areas of regions, and so on.* L, M, N *are the second fundamental coefficients reflecting the local warping of the surface, namely its deviation from the tangent plane at the point under consideration* (*Liseikin* 2004; *Toponogov* 2006). $\Gamma^1_{11}, \Gamma^2_{11}, \Gamma^1_{22}, \Gamma^2_{22}, \Gamma^1_{12}, \Gamma^2_{12}$ *are the Christoffel symbols, which depend only on the first fundamental coefficients* E, F, G*and their derivatives. The first three equations of (1) are known as Gauss equations and the last two are called Weingarten equations. Somasundaram* (2005) *has shown that Weingarten equations are supposed to be complementary to Gauss equations and Gauss equations are known as the partial differential equations of the surface theory.*

In terms of the fundamental theorem of surfaces, the first and second fundamental coefficients must satisfy the Gauss equations for defining a surface. So, the main task of HASM is to solve these Gauss equations:

$$\begin{cases} f_{xx} = \Gamma_{11}^1 f_x + \Gamma_{11}^2 f_y + \frac{L}{\sqrt{E+G-1}} \\ f_{yy} = \Gamma_{22}^1 f_x + \Gamma_{22}^2 f_y + \frac{N}{\sqrt{E+G-1}} \\ f_{xy} = \Gamma_{12}^1 f_x + \Gamma_{12}^2 f_y + \frac{M}{\sqrt{E+G-1}} \end{cases} . \tag{3}$$

Former researches (Yue et al. 2007, 2010a,b) have shown that different combinations of the equations in the equation set (3) result in different results based on simulation accuracy. Moreover, numerical problems will arise when the third equation in Gauss equations is included in HASM (Yue 2011). Previous studies also indicated that the best combination with the least error, namely HASM4, is as follows (Yue et al. 2007):

$$\begin{cases} f_{xx} = \Gamma_{11}^1 f_x + \Gamma_{11}^2 f_y + \frac{L}{\sqrt{E+G-1}} \\ f_{yy} = \Gamma_{22}^1 f_x + \Gamma_{22}^2 f_y + \frac{N}{\sqrt{E+G-1}} \end{cases} . \tag{4}$$

Let $\{(x_i, y_j)|0 \le i \le I+1, 0 \le j \le J+1\}$ be the computational grids and h be the grid size in x and y directions. Finite difference methods are used for solving these differential equations. The discrete forms of f_x, f_y, f_{xx} and f_{yy} are as follows,

$$(f_x)_{(i,j)} \approx \begin{cases} \frac{f_{1,j}-f_{0,j}}{h} & i=0 \\ \frac{f_{i+1,j}-f_{i-1,j}}{2h} & i=1,\ldots,I, \\ \frac{f_{I+1,j}-f_{I,j}}{h} & i=I+1 \end{cases} \quad (f_{xx})_{(i,j)} \approx \begin{cases} \frac{f_{0,j}-2f_{1,j}+f_{2,j}}{h^2} & i=0 \\ \frac{f_{i-1,j}-2f_{i,j}+f_{i+1,j}}{h^2} & i=1,\ldots,I \\ \frac{f_{I+1,j}-2f_{I,j}+f_{I-1,j}}{h^2} & i=I+1 \end{cases}$$

$$(f_y)_{(i,j)} \approx \begin{cases} \frac{f_{i,1}-f_{i,0}}{h} & j=0 \\ \frac{f_{i,j+1}-f_{i,j-1}}{2h} & j=1,\ldots,J, \\ \frac{f_{i,J+1}-f_{i,J}}{h} & j=J+1 \end{cases} \quad (f_{yy})_{(i,j)} \approx \begin{cases} \frac{f_{i,0}-2f_{i,1}+f_{i,2}}{h^2} & j=0 \\ \frac{f_{i,j-1}-2f_{i,j}+f_{i,j+1}}{h^2} & j=1,\ldots,J \\ \frac{f_{i,J+1}-2f_{i,J}+f_{i,J-1}}{h^2} & j=J+1 \end{cases}$$

Correspondingly, Eq. (4) can be approximated by

$$\begin{cases} \frac{f_{i+1,j}^{n+1}-2f_{i,j}^{n+1}+f_{i-1,j}^{n+1}}{h^2} = (\Gamma_{11}^1)_{i,j}^n \frac{f_{i+1,j}^n-f_{i-1,j}^n}{2h} + (\Gamma_{11}^2)_{i,j}^n \frac{f_{i,j+1}^n-f_{i,j-1}^n}{2h} + \frac{L_{i,j}^n}{\sqrt{E_{i,j}^n+G_{i,j}^n-1}} \\ \frac{f_{i,j+1}^{n+1}-2f_{i,j}^{n+1}+f_{i,j-1}^{n+1}}{h^2} = (\Gamma_{22}^1)_{i,j}^n \frac{f_{i+1,j}^n-f_{i-1,j}^n}{2h} + (\Gamma_{22}^2)_{i,j}^n \frac{f_{i,j+1}^n-f_{i,j-1}^n}{2h} + \frac{N_{i,j}^n}{\sqrt{E_{i,j}^n+G_{i,j}^n-1}} \end{cases} , \tag{5}$$

where, n represents the number of iterations.

$$E_{i,j}^n = 1 + \left(\frac{f_{i+1,j}^n - f_{i-1,j}^n}{2h}\right)^2,$$

$$F_{i,j}^n = \left(\frac{f_{i+1,j}^n - f_{i-1,j}^n}{2h}\right)\left(\frac{f_{i,j+1}^n - f_{i,j-1}^n}{2h}\right),$$

$$
\begin{aligned}
G_{i,j}^n &= 1+\left(\frac{f_{i,j+1}^n - f_{i,j-1}^n}{2h}\right)^2,\\
L_{i,j}^n &= \frac{\frac{f_{i-1,j}^n - 2f_{i,j}^n + f_{i+1,j}^n}{h^2}}{\sqrt{1+\left(\frac{f_{i+1,j}^n - f_{i-1,j}^n}{2h}\right)^2+\left(\frac{f_{i,j+1}^n - f_{i,j-1}^n}{2h}\right)^2}}\\
N_{i,j}^n &= \frac{\frac{f_{i,j-1}^n - 2f_{i,j}^n + f_{i,j+1}^n}{h^2}}{\sqrt{1+\left(\frac{f_{i+1,j}^n - f_{i-1,j}^n}{2h}\right)^2+\left(\frac{f_{i,j+1}^n - f_{i,j-1}^n}{2h}\right)^2}},\\
(\Gamma_{11}^1)_{i,j}^n &= \frac{G_{i,j}^n(E_{i+1,j}^n - E_{i-1,j}^n)h - 2F_{i,j}^n(F_{i+1,j}^n - F_{i-1,j}^n)h + F_{i,j}^n(E_{i,j+1}^n - E_{i,j-1}^n)h}{4(E_{i,j}^n G_{i,j}^n - (F_{i,j}^n)^2)h^2},\\
(\Gamma_{22}^1)_{i,j}^n &= \frac{2G_{i,j}^n(F_{i,j+1}^n - F_{i,j-1}^n)h - G_{i,j}^n(G_{i+1,j}^n - G_{i-1,j}^n)h - F_{i,j}^n(G_{i,j+1}^n - G_{i,j-1}^n)h}{4(E_{i,j}^n G_{i,j}^n - (F_{i,j}^n)^2)h^2},\\
(\Gamma_{11}^2)_{i,j}^n &= \frac{2E_{i,j}^n(F_{i+1,j}^n - F_{i-1,j}^n)h - E_{i,j}^n(E_{i,j+1}^n - E_{i,j-1}^n)h - F_{i,j}^n(E_{i,j+1}^n - E_{i,j-1}^n)h}{4(E_{i,j}^n G_{i,j}^n - (F_{i,j}^n)^2)h^2},\\
(\Gamma_{22}^2)_{i,j}^n &= \frac{E_{i,j}^n(G_{i,j+1}^n - G_{i,j-1}^n)h - 2F_{i,j}^n(F_{i,j+1}^n - F_{i,j-1}^n)h + F_{i,j}^n(G_{i+1,j}^n - G_{i-1,j}^n)h}{4(E_{i,j}^n G_{i,j}^n - (F_{i,j}^n)^2)h^2}.
\end{aligned}
$$

The matrix formulation of Eq. (5) can be expressed as,

$$
\begin{cases} Ax^{n+1} = d^n \\ Bx^{n+1} = q^n \end{cases}, \tag{6}
$$

where $x^{n+1} = (f_{1,1}^{n+1}, \ldots, f_{1,J}^{n+1}, f_{2,1}^{n+1}, \ldots, f_{2,J}^{n+1}, \ldots, f_{I-1,1}^{n+1}, \ldots, f_{I-1,J}^{n+1}, f_{I,1}^{n+1}, \ldots, f_{I,J}^{n+1})^T$,

$$
A = \begin{bmatrix} -2I & I & & & \\ I & -2I & I & & \\ & \ddots & \ddots & \ddots & \\ & & I & -2I & I \\ & & & I & -2I \end{bmatrix}_{I\cdot J\times I\cdot J}, \quad I = \begin{bmatrix} 1 & & \\ & \ddots & \\ & & 1 \end{bmatrix}_{J\times J}.
$$

$$
B = \begin{bmatrix} \widehat{B} & & \\ & \ddots & \\ & & \widehat{B} \end{bmatrix}_{I\cdot J\times I\cdot J}, \quad \widehat{B} = \begin{bmatrix} -2 & 1 & & & & & \\ 1 & -2 & 1 & & & & \\ & \ddots & \ddots & \ddots & & & \\ & & 1 & -2 & 1 & & \\ & & & \ddots & \ddots & \ddots & \\ & & & & 1 & -2 & 1 \\ & & & & & 1 & -2 \end{bmatrix}_{J\times J},
$$

A and B denote the coefficient matrices of Eq. (5) and d, q are the right-hand vectors of Eq. (5), respectively. The boundary value of HASM4 is obtained by other surface modeling methods.

Be themselves, Eq. (4) do not determine unique solution function, in general, provided f is sufficiently smooth. To single out particular solution, value z_0 of solution function must be specified at some point (x_0, y_0). The following equality-constrained least squares problem is developed to make the interpolated values equal to or approximate to the sampled values at the sampling points,

$$\begin{cases} \min \left\| \begin{bmatrix} A \\ B \end{bmatrix} x^{n+1} - \begin{bmatrix} d \\ q \end{bmatrix}^n \right\|_2 , \\ Sx^{n+1} = k \end{cases} \tag{7}$$

where $S(l, (i-1) \cdot J + j) = 1$, $k(l) = \overline{f}_{i,j}$, this means the sampled value is $\overline{f}_{i,j}$ at the lth sampling point (x_i, y_j).

An interesting way to obtain an approximate solution to (7) is to solve the unconstrained least squares problem

$$\min_x \left\| \begin{bmatrix} A \\ B \\ \lambda S \end{bmatrix} x^{n+1} - \begin{bmatrix} d \\ q \\ \lambda k \end{bmatrix}^n \right\| . \tag{8}$$

For a suitable λ (Bjorck 1968; Golub and Van Loan 2009), this problem (8) is equivalent to the symmetric positive definite linear system

$$Wx^{n+1} = v^n, \tag{9}$$

where $W = A^T A + B^T B + \lambda^2 S^T S$, $v = A^T d + B^T q + \lambda^2 S^T k$, λ is the weight of the sampling points. For large values of λ, however, numerical problems arise (Golub and Van Loan 2009). Fortunately, we found that the simulation accuracy of HASM is less sensitive to the selection of λ when the value of it is between 1 and 10. In addition, the accuracy decreases if λ is larger than 10. Since λ affects the contribution of the sampling points to the simulated surface, in a complex region, a smaller value of λ is selected and a bigger value is selected in a flat region (Chen and Yue 2010).

Modified Gauss–Seidel method (MGS), preconditioned conjugate gradient method (PCG), adaptive method (AM) and multi-grid method (MG) have been used to solve the linear system (9) (Yue et al. 2010a,b; Yue 2011; Chen et al. 2012). Results show that AM is the fastest method and uses minimum storage space compared to other methods. The method with the highest accuracy, however, is PCG method (Yue 2011). With the development of the high performance computing, more attention has been paid to simulation accuracy rather than computing speed and memory usage. Therefore, we use PCG method to solve the linear system in this study.

3 Modifications of HASM

Somasundaram (2005) has shown that Gauss equations are the partial differential equations of the surface theory while Weingarten equations are the supplement to Gauss equations. Based on this, HASM4 takes into account only the Gauss equations, but without considering the mixed derivatives $f_{xy} = \Gamma_{12}^1 f_x + \Gamma_{12}^2 f_y + \frac{M}{\sqrt{E+G-1}}$ of this equation set (Yue 2011), which doesn't follow the content of the surface theory. Next, we add this equation into HASM4 to give a modified version of it, which first ensures that HASM is integral theoretically.

Consider the following Gauss equations (3),

$$\begin{cases} f_{xx} = \Gamma_{11}^1 f_x + \Gamma_{11}^2 f_y + \frac{L}{\sqrt{E+G-1}} \\ f_{yy} = \Gamma_{22}^1 f_x + \Gamma_{22}^2 f_y + \frac{N}{\sqrt{E+G-1}} \\ f_{xy} = \Gamma_{12}^1 f_x + \Gamma_{12}^2 f_y + \frac{M}{\sqrt{E+G-1}} \end{cases}.$$

In the development of HASM (HASM2), researchers have considered the third equation in Gauss equations (Yue and Du 2006), and for the inner grid points, the discrete scheme of f_{xy} in HASM2 is

$$(f_{xy})_{(i,j)} = \frac{f_{i+1,j+1} - f_{i-1,j+1} + f_{i-1,j-1} - f_{i+1,j-1}}{4h^2}, \quad i = 1, \ldots, I, \;\; j = 1, \ldots, J.$$

For the boundary points, the discrete value of f_{xy} is the initial value at the corresponding point. However, this discrete form of f_{xy} leads to algebraic systems with loss of diagonal dominance and thus computational complexity, which eventually leads to a stack overflow in HASM2 simulation (Yue 2011). We now form the following type of difference:

$$(f_{xy})_{(i,j)} = \begin{cases} \frac{f_{1,1}-f_{1,0}-f_{0,1}+f_{0,0}}{h^2} & i=0,\ j=0 \\ \frac{f_{1,J+1}-f_{1,J}-f_{0,J+1}+f_{0,J}}{h^2} & i=0,\ j=J+1 \\ \frac{f_{1,j+1}-f_{0,j+1}-f_{1,j-1}+f_{0,j-1}}{2h^2} & i=0,\ j=1,\ldots,J \\ \frac{f_{I+1,1}-f_{I,0}-f_{I,1}+f_{I+1,0}}{h^2} & i=I+1,\ j=0 \\ \frac{f_{I,J}-f_{I+1,J}-f_{I,J+1}+f_{I+1,J+1}}{h^2} & i=I+1,\ j=J+1 \\ \frac{f_{I+1,j+1}-f_{I,j+1}-f_{I+1,j-1}+f_{I,J-1}}{2h^2} & i=I+1,\ j=1,\ldots,J \\ \frac{f_{i+1,1}-f_{i+1,0}-f_{i-1,1}+f_{i-1,0}}{2h^2} & i=1,\ldots,I,\ j=0 \\ \frac{f_{i+1,J+1}-f_{i+1,J}-f_{i-1,J+1}+f_{i-1,J}}{2h^2} & i=1,\ldots,I,\ j=J+1 \\ \frac{f_{i+1,j+1}-f_{i+1,j}-f_{i,j+1}+2f_{i,j}-f_{i-1,j}-f_{i,j-1}+f_{i-1,j-1}}{2h^2} & i=1,\ldots,I,\ j=1,\ldots,J. \end{cases}$$

For the inner point (x_i, y_j), this formulation of derivative makes full use of the information at this point and restores diagonal dominance (Karniadakis and Kirby 2003). Therefore, the equations of the modified version of HASM are as follows:

$$\begin{cases} \frac{f_{i+1,j}^{n+1}-2f_{i,j}^{n+1}+f_{i-1,j}^{n+1}}{h^2} = (\Gamma_{11}^1)_{i,j}^n \frac{f_{i+1,j}^n-f_{i-1,j}^n}{2h} + (\Gamma_{11}^2)_{i,j}^n \frac{f_{i,j+1}^n-f_{i,j-1}^n}{2h} + \frac{L_{i,j}^n}{\sqrt{E_{i,j}^n+G_{i,j}^n-1}} \\ \frac{f_{i,j+1}^{n+1}-2f_{i,j}^{n+1}+f_{i,j-1}^{n+1}}{h^2} = (\Gamma_{22}^1)_{i,j}^n \frac{f_{i+1,j}^n-f_{i-1,j}^n}{2h} + (\Gamma_{22}^2)_{i,j}^n \frac{f_{i,j+1}^n-f_{i,j-1}^n}{2h} + \frac{N_{i,j}^n}{\sqrt{E_{i,j}^n+G_{i,j}^n-1}} \\ \frac{f_{i+1,j+1}^{n+1}-f_{i+1,j}^{n+1}-f_{i,j+1}^{n+1}+2f_{i,j}^{n+1}-f_{i-1,j}^{n+1}-f_{i,j-1}^{n+1}+f_{i-1,j-1}^{n+1}}{2h^2} = (\Gamma_{12}^1)_{i,j}^n \frac{f_{i+1,j}^n-f_{i-1,j}^n}{2h} + (\Gamma_{12}^2)_{i,j}^n \\ \qquad \frac{f_{i,j+1}^n-f_{i,j-1}^n}{2h} + \frac{M_{i,j}^n}{\sqrt{E_{i,j}^n+G_{i,j}^n-1}} \end{cases} \tag{10}$$

where,

$$E_{i,j}^n = 1+\left(\frac{f_{i+1,j}^n-f_{i-1,j}^n}{2h}\right)^2,$$

$$F_{i,j}^n = \left(\frac{f_{i+1,j}^n-f_{i-1,j}^n}{2h}\right)\left(\frac{f_{i,j+1}^n-f_{i,j-1}^n}{2h}\right),$$

$$G_{i,j}^n = 1+\left(\frac{f_{i,j+1}^n-f_{i,j-1}^n}{2h}\right)^2,$$

$$L_{i,j}^n = \frac{\frac{f_{i-1,j}^n-2f_{i,j}^n+f_{i+1,j}^n}{h^2}}{\sqrt{1+\left(\frac{f_{i+1,j}^n-f_{i-1,j}^n}{2h}\right)^2+\left(\frac{f_{i,j+1}^n-f_{i,j-1}^n}{2h}\right)^2}},$$

$$N_{i,j}^n = \frac{\frac{f_{i,j-1}^n-2f_{i,j}^n+f_{i,j+1}^n}{h^2}}{\sqrt{1+\left(\frac{f_{i+1,j}^n-f_{i-1,j}^n}{2h}\right)^2+\left(\frac{f_{i,j+1}^n-f_{i,j-1}^n}{2h}\right)^2}},$$

$$M_{i,j}^n = \frac{\frac{f_{i+1,j+1}^n-f_{i+1,j}^n-f_{i,j+1}^n+2f_{i,j}^n-f_{i-1,j}^n-f_{i,j-1}^n+f_{i-1,j-1}^n}{2h^2}}{\sqrt{1+\left(\frac{f_{i+1,j}^n-f_{i-1,j}^n}{2h}\right)^2+\left(\frac{f_{i,j+1}^n-f_{i,j-1}^n}{2h}\right)^2}},$$

$$(\Gamma_{11}^1)_{i,j}^n = \frac{G_{i,j}^n(E_{i+1,j}^n-E_{i-1,j}^n)h-2F_{i,j}^n(F_{i+1,j}^n-F_{i-1,j}^n)h+F_{i,j}^n(E_{i,j+1}^n-E_{i,j-1}^n)h}{4(E_{i,j}^nG_{i,j}^n-(F_{i,j}^n)^2)h^2},$$

$$(\Gamma_{22}^1)_{i,j}^n = \frac{2G_{i,j}^n(F_{i,j+1}^n-F_{i,j-1}^n)h-G_{i,j}^n(G_{i+1,j}^n-G_{i-1,j}^n)h-F_{i,j}^n(G_{i,j+1}^n-G_{i,j-1}^n)h}{4(E_{i,j}^nG_{i,j}^n-(F_{i,j}^n)^2)h^2},$$

$$(\Gamma_{11}^2)_{i,j}^n = \frac{2E_{i,j}^n(F_{i+1,j}^n-F_{i-1,j}^n)h-E_{i,j}^n(E_{i,j+1}^n-E_{i,j-1}^n)h-F_{i,j}^n(E_{i,j+1}^n-E_{i,j-1}^n)h}{4(E_{i,j}^nG_{i,j}^n-(F_{i,j}^n)^2)h^2},$$

$$(\Gamma_{22}^2)_{i,j}^n = \frac{E_{i,j}^n(G_{i,j+1}^n-G_{i,j-1}^n)h-2F_{i,j}^n(F_{i,j+1}^n-F_{i,j-1}^n)h+F_{i,j}^n(G_{i+1,j}^n-G_{i-1,j}^n)h}{4(E_{i,j}^nG_{i,j}^n-(F_{i,j}^n)^2)h^2},$$

$$(\Gamma_{12}^2)_{i,j}^n = \frac{E_{i,j}^n(G_{i+1,j}^n-G_{i-1,j}^n)h-F_{i,j}^n(E_{i,j+1}^n-E_{i,j-1}^n)h}{4(E_{i,j}^nG_{i,j}^n-(F_{i,j}^n)^2)h^2},$$

$$(\Gamma_{12}^1)_{i,j}^n = \frac{G_{i,j}^n(E_{i+1,j}^n-E_{i-1,j}^n)h-F_{i,j}^n(G_{i+1,j}^n-G_{i-1,j}^n)h}{4(E_{i,j}^nG_{i,j}^n-(F_{i,j}^n)^2)h^2}.$$

Then, just as in HASM4, the constraint equation about sample point information is added to Eq. (10) and the formulation of Mod.HASM can be expressed as,

$$\begin{cases} \min \left\| \begin{bmatrix} A \\ B \\ C \end{bmatrix} z^{n+1} - \begin{bmatrix} d \\ q \\ p \end{bmatrix}^{n} \right\|, \\ s.t.\ Sz^{(n+1)} = k \end{cases} \tag{11}$$

where, $A = \begin{bmatrix} -2I & I & & & & \\ I & -2I & I & & & \\ & \ddots & \ddots & \ddots & & \\ & & & I & -2I & I \\ & & & & I & -2I \end{bmatrix}_{(I+2)\cdot(J+2)\times(I+2)\cdot(J+2)}$, $I = \begin{bmatrix} 1 & & \\ & \ddots & \\ & & 1 \end{bmatrix}_{(J+2)\times(J+2)}$

$$B = \begin{bmatrix} \widetilde{B} & & \\ & \ddots & \\ & & \widetilde{B} \end{bmatrix}_{(I+2)\cdot(J+2)\times(I+2)\cdot(J+2)}, \quad \widetilde{B} = \begin{bmatrix} -2 & 1 & & & & & \\ 1 & -2 & 1 & & & & \\ & \ddots & \ddots & \ddots & & & \\ & & 1 & -2 & 1 & & \\ & & & \ddots & \ddots & \ddots & \\ & & & & 1 & -2 & 1 \\ & & & & & 1 & -2 \end{bmatrix}_{(J+2)\times(J+2)},$$

$$C = \begin{bmatrix} C_1 & -C_1 & & & \\ C_3 & C_2 & C_4 & & \\ & \ddots & \ddots & \ddots & \\ & & C_3 & C_2 & C_4 \\ & & & C_1 & -C_1 \end{bmatrix}_{(I+2)\cdot(J+2)\times(I+2)\cdot(J+2)}, \quad C_1 = \begin{bmatrix} 1 & -1 & & & \\ 1/2 & 0 & -1/2 & & \\ & \ddots & \ddots & \ddots & \\ & & 1/2 & 0 & -1/2 \\ & & & 1 & -1 \end{bmatrix}_{(J+2)\times(J+2)}$$

$$C_2 = \begin{bmatrix} 0 & 0 & 0 & & \\ -1/2 & 1 & -1/2 & & \\ & \ddots & \ddots & \ddots & \\ & & -1/2 & 1 & -1/2 \\ & & 0 & 0 & 0 \end{bmatrix}_{(J+2)\times(J+2)}, \quad C_3 = \begin{bmatrix} 1/2 & -1/2 & & & \\ 1/2 & -1/2 & & & \\ & \ddots & \ddots & & \\ & & 1/2 & -1/2 & \\ & & & 1/2 & -1/2 \end{bmatrix}_{(J+2)\times(J+2)}$$

$$C_4 = \begin{bmatrix} -1/2 & 1/2 & & & \\ & -1/2 & 1/2 & & \\ & & \ddots & \ddots & \\ & & & -1/2 & 1/2 \\ & & & -1/2 & 1/2 \end{bmatrix}_{(J+2)\times(J+2)}.$$

A, B, C are the left hand sides of Eq. (10), respectively. The structures of A, B, S, k are the same in HASM4 and Mod.HASM, but the dimensions are different.

By introducing a suitable parameter λ, we finally get the matrix equation of Mod.HASM,

$$\overline{A}x^{n+1} = \overline{b}^{n}, \tag{12}$$

where, $\overline{A} = A^T A + B^T B + C^T C + \lambda^2 S^T S$ reflects the local relationship between each grid point and the surrounding points since $\overline{A}$ is a sparse matrix of which the nonzero elements in each row denote the coefficients of the relationship. $\overline{b} = A^T d + B^T q + C^T p + \lambda^2 S^T k$ is the right-hand vector and x is a vector that each element denotes the simulated value of the corresponding grid point.

4 Numerical and real-world tests

In this section, we first take Gauss synthetic surface as the test surface to test the performance of the modified version so that the true value is able to be predetermined to avoid the uncertainty caused by uncontrollable data errors. Since air temperature is the necessary input for sound agricultural planning, the second part of this section applies Mod.HASM and HASM4 to simulate annual mean temperature of China for the considered temporal period (1951–2010).

4.1 Numerical tests

Gauss synthetic surface is expressed as:

$$f(x, y) = 3(1-x)^2 e^{-x^2-(y+1)^2} - 10\left(\frac{x}{5} - x^3 - y^5\right) e^{-x^2-y^2} - \frac{e^{-(x+1)^2-y^2}}{3},$$

the computational domain is $[-3, 3] \times [-3, 3]$.

Root mean square error (RMSE) is used to evaluate the performance of Mod.HASM and HASM4. The formulation of RMSE is

$$RMSE = \sqrt{\frac{\sum_{k=1}^{N} (f_k - \overline{f}_k)^2}{N}},$$

where f_k is the true value at the kth point (x_i, y_j); $\overline{f}_k$ is the simulated value; $N$is the number of validation points. The value of this criterion should be close to zero if the method is accurate.

For different h, we then compare the performances of HASM4, Mod.HASM, kriging, IDW and splines (Table 1). The outer iterative criterion is Gauss–Codazii equations and, for a fixed n, the inner stopping criterion of Eq. (12) is $\|\overline{b}^n - \overline{A}x^{n+1}\|_2 \leq 10^{-12}$.

A phenomenon that the accuracy of HASM4 is inferior to splines occurred in this case study when the grid number are 61×61, 301×301 and 601×601. Moreover,

Table 1 The values of RMSE for Mod.HASM, HASM4, kriging, IDW and splines

Grid numbers	61 × 61	301 × 301	601 × 601	1,201 × 1,201
Mod.HASM	0.0410	0.0135	0.0004	0.0001
HASM4	0.0979	0.0660	0.0022	0.0010
Kriging	0.1369	0.0830	0.0033	0.0015
IDW	0.3197	0.2316	0.0762	0.0750
Splines	0.0426	0.0171	0.0003	0.0629

Table 2 The CPU time (s) for Mod.HASM, HASM4, kriging, IDW and splines

Grid numbers	61 × 61	301 × 301	601 × 601	1,201 × 1,201
Mod.HASM	176	2,711	3,032	3,745
HASM4	62	398	406	489
Kriging	249	2,672	2,720	2,752
IDW	53	146	148	154
Splines	102	152	154	170

when the grid number are 601 × 601 and 1,201 × 1,201, the accuracy of HASM4 is slightly better than kriging method. However, for different computational scales, the simulation accuracy of Mod.HASM is much higher than HASM4 and other classical interpolation methods.

Table 2 gives the CPU time for each method. It should be noted that the required CPU times are significantly different for the above methods. The computational time for IDW is typically small, since it is easy to realize. Because of the computation of the semi-variogram, the computational time of kriging is large. Mod.HASM takes a longer time than HASM4 due to the more complex nonlinear system. Compared with other methods, Mod.HASM spends the most time expect for the case 61 × 61. Since the introduction of the third equation in Mod.HASM, the memory requirement of it is two times greater than that of HASM4. Compared with other methods, both HASM4 and Mod.HASM require large memory. However, Mod.HASM can be realized further in parallel to improve the efficiency of it.

4.2 A real word example

Sixty (1951–2010) years annual mean temperature data from 711 meteorological stations in China are interpolated. Figure 1 shows the distribution of the meteorological stations. We compare the performance of HASM4, Mod.HASM and those of kriging, IDW, and splines method. These classical methods are performed using the module of 3D analyst ArcGIS 10.1. We compare different parameters for kriging, IDW and splines and decide the best parameters for each technique with the smallest RMSE values. For kriging, the exponential, spherical, Gaussian and linear model are fitted to the experimental variogram and the number of the closest samples chosen varied from 5 to 30. We find that, in all implementations of kriging, the Gaussian semivariogram model with 16 samples provides the overall best results. IDW is estimated with powers of 1, 2, 3 and 4. The lowest RMSE value for IDW is found with a neighborhood of 16 points and power of one. For splines, the regularized and tension methods are implemented using the same neighborhood variations as used in kriging and IDW. The best result for splines is provided using tension method with eighteen neighborhood points.

The climate data are divided into two groups: we select at random 85 % of them to interpolate the temperature surface, while we use the remaining 15 % for validation. Three indices: RMSE, MAE and MRE are calculated from the station values and interpolated values at each validation sample site. The formulations of MAE and MRE are:

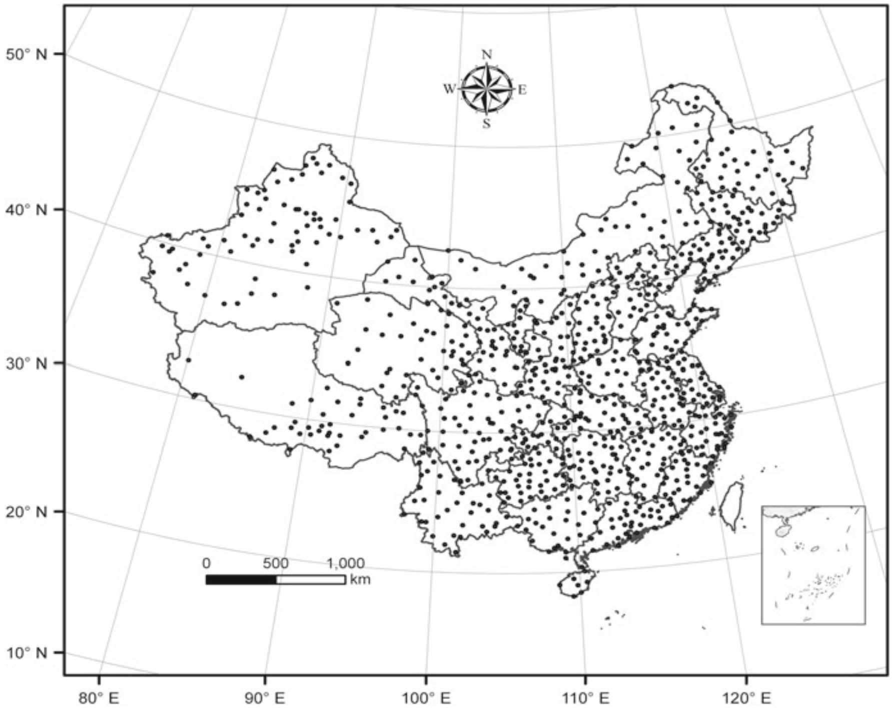

Fig. 1 Location of meteorological stations

$$MAE = \sum_{k=1,\ldots,N} \frac{\left|f_k - \overline{f}_k\right|}{N}, \quad MRE = \sum_{k=1,\ldots,N} \frac{\left|f_k - \overline{f}_k\right|}{f_k N},$$

where f_k, $\overline{f}_k$ and N have the same meanings as in RMSE.

Yue (2011) has shown that the larger the ratio between sampled points and grid points, the smaller the simulation error of HASM. Since we just compare the simulation accuracy of different methods under the same conditions, we fix the grid number based on the studied area and the distribution of the meteorological stations. Then, a cell size of 10×10 km is chosen in this research. Correspondingly, the values of I, J in x and y are 405 and 485, respectively. Results show that the computational time for IDW is 143 seconds. For splines, kriging, HASM4 and Mod.HASM, the computational times are 159, 2,602, 506, and 3,079 s, respectively. IDW takes the least time while Mod.HASM spends the most. However, the results of the accuracy tests (Table 3)

Table 3 The means of MAEs, MREs and RMSEs of 20 validation sets for Mod.HASM, HASM4, kriging, IDW and splines

Methods	Mod.HASM	HASM4	Kriging	IDW	Splines
MAE	1.1571	1.3109	1.3205	1.3472	1.4661
MRE	0.1731	0.2061	0.2336	0.2688	0.3927
RMSE	1.8283	2.0856	2.0990	2.1142	2.1117

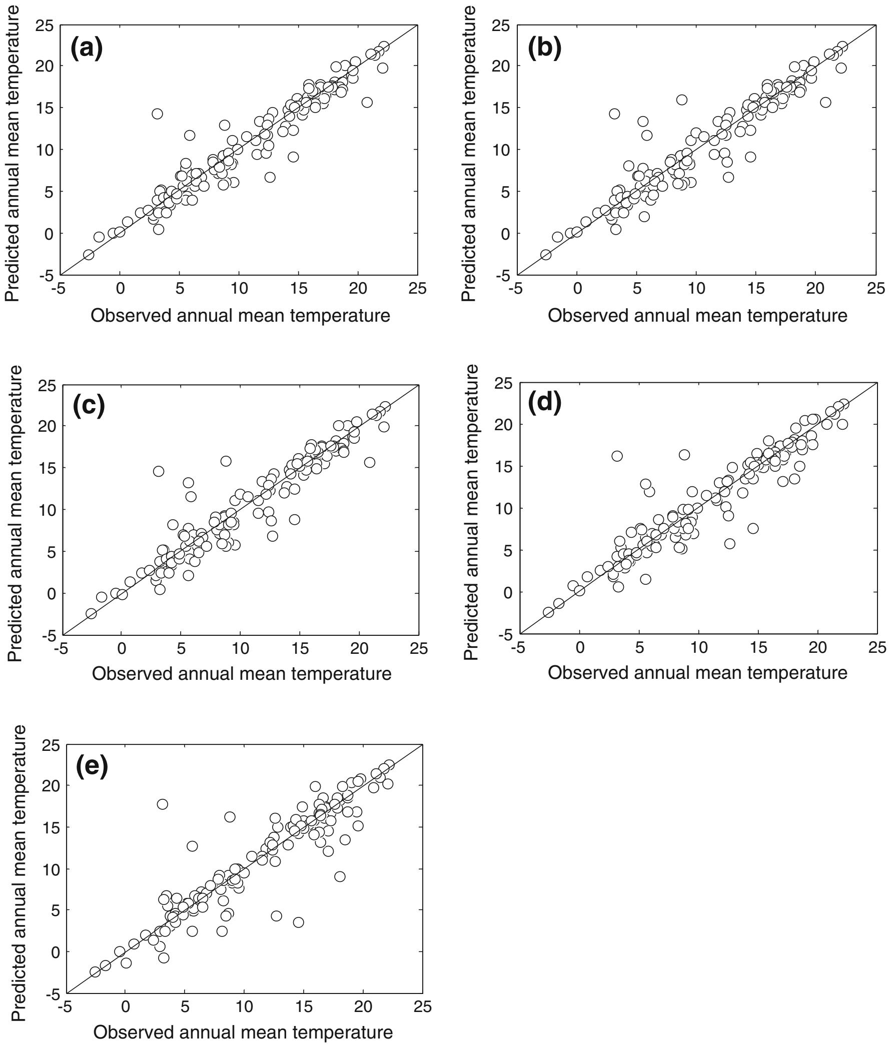

Fig. 2 Estimated versus observed annual mean temperature (°C). **a** Mod.HASM; **b** HASM4; **c** Kriging; **d** IDW; **e** Splines

show that Mod.HASM produces the most accurate interpolated temperature data. The differences between the MAE, MRE and RMSE values of HASM4 and those of kriging are slight. For annual mean temperature, the results of HASM4, kriging and IDW methods show very small differences, while splines displays the largest MAE and MRE values. Through comparing with other methods, Mod.HASM is the optimum spatial interpolation method for the annual mean temperature based on the validation results.

Figure 2 shows the estimated values of annual mean temperature against the observations. The straight line represents the best fit. Mod.HASM estimates the annual mean temperature quite reliably as is shown in this figure. Many simulation points are relatively far from the straight line of $y = x$ by using other methods including HASM4. The correlation coefficient between predicted and observed values is 0.95 for Mod.HASM and 0.94 for HASM4. The correlation coefficients are 0.94, 0.93 and 0.91 for kriging, IDW and splines, respectively. This analysis also indicates that Mod.HASM simulation has the highest accuracy.

Ninyerola et al. (2007) state that all models do substantially worse when the interpolation method does not use geographical information. The effects of many geographical and topographical factors on climate parameters are evaluated by several researchers (Ninyerola et al. 2007; Apaydin et al. 2011; Samanta et al. 2012). Many studies show that method of 'multiple regression plus space residual error' is better than that of 'directly interpolated for observe data of temperature' (Kurtzman and Kadmon 1999; Liao and Li 2004; Ninyerola et al. 2007; Joly et al. 2011). Since the purpose of this section is to test the effectiveness of Mod.HASM, more accurate products can be obtained using 'multiple regression plus space residual error' method.

5 Conclusions and discussion

5.1 Conclusions

Based on the fundamental theorem of surface theory, an improved version of HASM, Mod.HASM, is presented and validated by numerical and real world examples. The modified HASM is compared with the previous version and also with other classical interpolation methods: kriging, IDW, and splines. Both numerical and real world tests reveal that the interpolation accuracy of Mod.HASM is higher than HASM4 and other classical interpolation methods. Another important feature of Mod.HASM is that it is theoretically perfect which insures the good performance of this method.

5.2 Discussion

Kriging results rely heavily on a previously well-chosen semivariogram, which is difficult to estimate and validate against a true covariance function. Besides, kriging method generally assumes normally distributed variables which is difficult to satisfy in practical applications (Goovaerts 1999). Another frequently used model in spatial interpolation is the IDW method. There are no assumptions required of the input data for the application of IDW. However, IDW relies mainly on the inverse of the distance raised to the power and also be controlled by limiting the input points for calculating each interpolated point. The output surface of IDW is sensitive to clustering and the presence of outliers (Hartkamp et al. 1999). And splines estimates values using a mathematical function that minimizes overall surface curvature, resulting in a smooth surface. However, this method tends to generate steep gradients in data-poor areas leading to compounded errors in the estimation process (Wang 2006).

HASM4 ignores the second fundamental coefficient M while Mod.HASM is theoretically perfect, which insures that it performs best and improves HASM's simulation skills. In addition, the difference scheme for the mixed derivative f_{xy} used in this study avoids several numerical problems and substantial computational complexity (Karniadakis and Kirby 2003). For the available sampling information, although our tests show that Mod.HASM usually takes larger time than other methods, Mod.HASM can be improved further by adopting a parallel computing scheme.

For end-users, there are some places that need to be considered. The first one is the parameter λ. Since λ determines the contribution of the sampling points to the simulated surface, for mathematical surfaces, the most commonly used value for λ is 2 and the value of it ranges from 1 to 10 in real life applications. The selection of λ, however, is just based on experiences of the past. Further researches will be carried out about the choice of λ using some relevant theories of inverse and ill-posed problems. The optimal value of it can be obtained by using generalized cross validation method (GCV), as mentioned in Hancock and Hutchinson (2006). Other methods for finding the optimal λ can be found in Golub and Van Loan (1989), Brezinski et al. (2008), and Reichel et al. (2009), and so on. The second is the choice of the number of the grid points I, J in x and y directions. These can be determined by the studied area and the available sampled points. The optimal situation is that there is at least one sampled point in each grid. However, it is difficult to get enough sampled points in practice. Fortunately, for a particular application, an interesting phenomenon is found that when the sampling ratio is larger than a certain threshold, the simulation accuracy improves slowly, which indicates that the impact of the sampling density is limited. Therefore, to determine the values of I and J, we should find the threshold value for a given application through continuous tests.

To make the process of HASM4 and Mod.HASM easier, the grid size h is the same in the whole process. It seems better to make it changeable based on the studied area. Yue et al. (2010a,b) and Yue (2011) have shown that the adaptive refinement technique is very successful in reducing the computational and storage requirement for solving the partial differential equations of HASM. However, studies also show that the computational accuracy of it is lower than PCG method because of the subjectivity of the choice of the step size. Potentially, one may consider the finite-difference formula of higher order with the adaptive choice of h, as suggested in Naumova et al. (2012), for example. Mod.HASM in this study can be developed further to realize in the parallel environment with this adaptive technique when the grid resolution at the initial iteration is selected properly.

References

Apaydin, H., Anli, A.S., Ozturk, F.: Evaluation of topographical and geographical effects on some climatic parameters in the Central Anatolis Region of Turkey. Int. J. Climatol. **31**, 1264–1279 (2011)

Bjorck, A.: Iterative refinement of linear least squares solutions II. BIT **8**, 8–30 (1968)

Brezinski, C., Rodriguez, G., Seatzu, S.: Error estimates for linear systems with applications to regularization. Numer. Algorithm **49**, 85–104 (2008)

Carmo, M.P.: Differential Geometry of Curves and Surfaces. China Machine Press, Beijing (2006)

Chen, C.F., Yue, T.X.: A method of DEM construction and related error analysis. Comput. Geosci. **36**, 717–725 (2010)

Chen, C.F., Yue, T.X., Li, Y.Y.: A high speed method of SMTS. Comput. Geosci. **41**, 64–71 (2012)

Crain, I.K.: Digital representation of topographic surface. Photogramm Eng. Remote Sens **54**, 1577 (1970)

Golub, G.H., Van Loan, C.F.: Matrix Computation, Johns Hopkins Series in the Mathematical Sciences, 3rd edn. Johns Hopkins University Press, Baltimore (1989)

Golub, G.H., Van Loan, C.F.: Matrix Computations. Posts & Telecom Press, Beijing (2009)

Goovaerts, P.: Geostatistics in soil science: state-of-the-art and perspectives. Geoderma **89**, 1–45 (1999)

Hancock, P.A., Hutchinson, M.F.: Spatial interpolation of large climate data sets using bivariate thin plate smoothing splines. Environ. Model. Softw. **21**, 1684–1694 (2006)

Hartkamp, A.D., De Beurs, K., Stein, A., White, J.W.: Interpolation techniques for climate variables. NRG-GIS Series 99-01, CIMMYT, Mexio (1999)

Henderson, D.W.: Differential Geometry. Prentice-Hall, London (1998)

Joly, D., Brossard, T., Cardot, H., Cavailhes, J., Hilal, M., Wavresky, P.: Temperature interpolation based on local information: the example of France. Int. J. Climatol. **31**, 2141–2153 (2011)

Karniadakis, G.E.M., Kirby, I.I.R.M.: Parallel Scientific Computing in C++ and MPI. Cambridge University Press, Cambridge (2003)

Kurtzman, D., Kadmon, R.: Mapping of temperature variables in Isreal: a comparison of different interpolation methods. Clim. Res. **13**, 33–43 (1999)

Li, Z.L., Zhu, Q.: Digital Elevation Model. Wuhan Technical University of Surveying and Mapping Press, Wuhan (2000)

Liao, S.B., Li, Z.H.: Some practical problems related to raserization of air temperature. Meteorol. Sci. Technol. **32**, 352–356 (2004) (in Chinese)

Liseikin, V.D.: A Computational Differential Geometry Approach to Grid Generation. Springer, Berlin (2004)

Naumova, V., Pereverzyev, S.V., Sivananthan, S.: Adaptive parameter choice for one-side finite difference schemes and its application in diabetes technology. J. Complexity **28**, 524–538 (2012)

Ninyerola, M., Pons, X., Roure, J.M.: Objective air temperature mapping for the Iberian Peninsula using spatial interpolation and GIS. Int. J. Climatol. **27**, 1231–1242 (2007)

Reichel, L., Rodriguez, G., Seatzu, S.: Error estimates for large-scale ill-posed problems. Numer. Algorithms **51**, 341–361 (2009)

Samanta, S., Pal, D.K., Lohar, D.: Interpolation of climate variables and temperature modeling. Theor. Appl. Climatol. **107**, 35–45 (2012)

Somasundaram, D.: Differential Geometry. Alpha Science International Ltd, Harrow (2005)

Stott, J.P.: Surface Modeling by Computer. Thomas Telford Ltd for the Institution of Civil Engineers, London (1977)

Su, B.Q., Hu, H.S.: Differential Geometry. People's Education Press, Beijing (1997). (in Chinese)

Toponogov, V.A.: Differential Geometry of Curves and Surfaces. Birkhaeuser Boston, New York (2006)

Wang, F.: Quantitative Methods and Applications in GIS. CRC Press, Boca Raton (2006)

Wise, S.: GIS data modeling-lessons from the analysis of DTMs. Int. J. Geogr. Inf. Sci. **14**, 313–318 (2000)

Yue, T.X.: Surface Modeling: High Accuracy and High Speed Methods. CRC Press, New York (2011)

Yue, T.X., Du, Z.P.: Numerical test for optimum formulation of high accuracy surface modeling. Geo Inf. Sci. **8**, 83–87 (2006) (in Chinese)

Yue, T.X., Wang, S.H.: Adjustment computation of HASM: a high-accuracy and high-speed method. Int. J. Geogr. Inf. Sci. **24**, 1725–1743 (2010)

Yue, T.X., Du, Z.P., Song, D.J., Gong, Y.: A new method of high accuracy surface modeling and its application to DEM construction. Geomorphology **91**, 161–172 (2007)

Yue, T.X., Chen, C.F., Li, B.L.: An adaptive method of high accuracy surface modeling and its application to simulating elevation surface. Trans. GIS **14**, 615–630 (2010a)

Yue, T.X., Song, D.J., Du, Z.P., Wang, W.: High accuracy surface modeling and its application to DEM generation. Int. J. Remote Sens. **31**, 2205–2226 (2010b)